Oceanologia, 68 (2)/2026, 68211
Polish Academy of Sciences
Institute of Oceanology

https://doi.org/10.5697/JWPI2821

Reconstruction of the South Java Coastal Current during the Indian Ocean Dipole and El Niño Southern Oscillation from 1993 to 2023

Martono[1,*], Noir P. Purba[3], Heru Santoso[1], Yosef Prihanto[1], Amaliah Nurlatifah[1], Teguh Harjana[1], Edy Maryadi[2]

Abstract
The South Java Coastal Current (SJCC) transports warm water from the tropical Indian Ocean toward the southeast along the coastal areas of western Sumatra and southern Java. This study aims to reconstruct the SJCC and examine its seasonal and interannual variations during different phases of the Indian Ocean Dipole (IOD) and El Niño–Southern Oscillation (ENSO) from 1993 to 2023. Surface ocean currents were examined using the Ocean Surface Current Analysis Real-time (OSCAR) dataset, along with sea level anomaly (SLA), ERA5 surface wind, Niño 3.4, and Dipole Mode Index (DMI). Results reveal that, on the intraseasonal timescale, the SJCC exhibits a dominant periodicity of about 76 days. In general, the eastward surface currents along the southern waters of Java are formed throughout the year. From June to September, the eastward surface currents are usually absent under normal conditions but appear during negative IOD and La Niña events, driven by wind mechanisms and Kelvin wave activity. Conversely, during positive IOD and El Niño events, the eastward surface currents weaken significantly or are suppressed, especially from October to January. The influence of IOD events on the eastward surface currents is stronger than that of ENSO. The variability of the eastward surface currents is affected not only by seasonal monsoon winds but also by large-scale ocean-atmosphere interactions and the movement of equatorial Kelvin waves. Understanding these processes is essential for more accurate prediction of regional circulation, heat transfer, and climate variability in the southeastern tropical Indian Ocean.

Keywords
Monsoon; Eastward currents; ENSO; IOD

[1] *Center for Climate and Atmospheric Research – Indonesian National Research and Innovation Agency, Bandung, Indonesia*
[2] *Research Centre for Artificial Intelligence and Cyber Security – Indonesian National Research and Innovation Agency, Bandung, Indonesia*
[3] *Department of Marine Science, Faculty of Fisheries and Marine Science, Padjadjaran University, Jatinangor, Indonesia*
***Correspondence**: mart001@brin.go.id (Martono)

Received: 28 June 2025; **revised:** 4 March 2026; **accepted**: 12 March 2026

1. Introduction

The dynamics of the waters south of Java, which form part of the southeastern tropical Indian Ocean, are highly complex and influenced by multiple key oceanographic factors (Wijffels et al., 1996; Pranowo et al., 2016; Ningsih et al., 2021). These dynamics result from the interaction between several currents, including the South Equatorial Current (SEC) and the SJCC (Wyrtki, 1961; Feng and Wijffels, 2002; Utamy et al., 2015), significant upwelling phenomena (Wyrtki, 1962; Susanto et al., 2001; Qu et al., 2005; Kuswardani and Qiao, 2014; Atmadipoera et al., 2020; Wirasatriya et al., 2020; Wen et al., 2023), and the IOD (Adiwira et al., 2018), which has substantial impacts on regional climate variability (Saji et al., 1999; Webster et al., 1999; Ashok et al., 2001). Additionally, the Indonesian Throughflow (ITF) serves as a major conduit for water mass exchange between the Pacific and Indian Oceans (Potemra, 1999; Wijffels et al., 2002; Gordon, 2005; Gordon et al., 2010; Sprintall et al., 2019; Jin and Wright, 2020), while the ENSO plays a crucial role in modulating both oceanic and atmospheric variability in this region (Susanto and Marra, 2005; Hood et al., 2015). Despite the importance of these processes, detailed investigations into the SJCC remain limited, including the characteristics during the IOD and ENSO. However, these phenomena significantly alter sea surface temperatures, wind patterns, and ocean

circulation.

SJCC is a predominantly eastward-flowing, coastally trapped current along the southern coast of Indonesia from Java to Sumba. Its variability is strongly influenced by remote equatorial forcing associated with the South Equatorial Counter Current (SECC), often transmitted via coastal Kelvin waves (Quadfasel and Cresswell, 1992; Utamy et al., 2015). However, there is considerable debate regarding the persistence of the SJCC. Some studies suggest that the SJCC forms only during the northwest monsoon, while others indicate it is a year-round phenomenon. This current system plays a significant role in heat and nutrient exchange between the central Indian Ocean and the waters along the southern Java and western Sumatra coasts. Studies have demonstrated that the SJCC influences the distribution of temperature, salinity, and nutrient concentrations in this region (Utamy et al., 2015). Additionally, the interaction between the SJCC and the ITF generates mesoscale eddies that exhibit both cyclonic and anticyclonic characteristics, with diameters ranging from 20 to 200 km (Tussadiah et al., 2016). Previous research has shown that, in addition to its predominant flow toward the Central Indian Ocean (CIO), the SJCC transports water masses from the Indian Ocean into the Indonesian Seas and the Banda Sea through various straits, such as the Sumba and Ombai Straits (Atmadipoera et al., 2022).

In terms of regional climate, the presence of the SJCC is critical in regulating sea surface temperature (SST) variability and atmospheric circulation over the Indonesian region. The warm water masses transported by the SJCC influence rainfall patterns and the formation of strong atmospheric convection, particularly during the northwest monsoon (Schott et al., 2009). This process contributes to the high precipitation intensity observed across Sumatra, Java, Bali, and Timor (Aldrian and Susanto, 2003). Notably, the increased precipitation during the northwest monsoon coincides with the development of the SJCC, highlighting a strong linkage between oceanic circulation and regional weather systems (Wu et al., 2013).

Given the critical role of the SJCC in modulating regional climate, ocean circulation, and marine ecosystems, this study aims to reconstruct the existence and variability of the SJCC under different climate conditions, including normal years and extreme IOD and ENSO events. Understanding these seasonal dynamics is essential for accurately predicting current behaviour, heat transport, and broader climatic implications. The findings from this research will provide a deeper understanding of ocean-climate interactions in the southeastern tropical Indian Ocean, thereby enhancing climate forecasting, fisheries management, and regional climate adaptation strategies. Moreover, understanding the SJCC's contribution to global thermohaline circulation will help improve global climate models and future climate variability predictions.

2. Material and methods

2.1 Geographic characteristics

The research location comprises the western part of Sumatra and the southern waters of Java extending to Sumba Island, which includes 13°S–4°S and 101°E–117°E (Figure 1). The region south of Java exhibits significant depth variation, ranging from shallow continental shelf areas near the island to the deepest parts of the Java trenches. The continental shelf extends from the coastline to depths of approximately 50–200 m, serving as an important region for coastal upwelling and marine productivity, particularly during the southeast monsoon (SEM) (Utamy et al., 2015). Beyond this, the continental slope rapidly descends to depths of 1,000–3,000 m, creating a transition zone where water mass mixing and thermohaline circulation occur.

From the surface to depths of almost 100 to 150 m, the South Java Current (SJC) flows along Java's southern coast over a width of 100 to 200 km. During monsoon seasons, this current reaches peak velocities of 0.5 to 1.0 m s^{-1}, and during transitional seasons it averages 0.2 to 0.4 m s^{-1} (Iskandar et al., 2006). The monsoon cycle controls its seasonal dynamics, and enhanced upwelling, caused by the SJC, flows westward during the SEM (June to September), decreasing surface temperature by 2 to 3°C and raises salinity (Purba and Khan, 2019). During this period, velocities might reach a maximum of 1.0 m s^{-1}. The SJC lasts 90 days. This water mass has a strong velocity in boreal winter (Michida and Yoritaka, 1996; Sprintall et al., 1999). Conversely, the Under-SJC, a subsurface current, exhibits a 60-day variant cycle influenced by the Madden-Julian Oscillation (MJO) and is driven by winds in the eastern equatorial Indian Ocean, particularly over Sumatra. Furthermore, the ITF waters create a relatively narrow and strong current flowing from the major exit channels throughout the tropical South Indian Ocean, specifically between 8 and 14°S. This current is part of the westward-flowing SEC. It consists of a well-defined low-salinity core of surface-to-thermocline water, as well as a second core at intermediate depths (600 to 1200 m) characterized by the lowest salinity and highest silica content.

2.2 Data and method

In this study, we used the Ocean Surface Current Analysis Real-time (OSCAR) dataset to analyze surface circulation dynamics and the RAMA dataset for OSCAR data verification. The OSCAR dataset is widely recognized for its ability to estimate near-surface geostrophic and geostrophic currents by incorporating satellite-derived sea level, wind stress, and sea surface currents. Several studies have validated OSCAR's accuracy, particularly in tropical and equatorial regions. For instance, Bonjean and Lagerloef (2002) introduced the OSCAR dataset and demonstrated its capability in diagnosing tropical Pacific Ocean currents. Similarly, Johnson et al. (2007) conducted extensive valida-

tion against in situ observations (moored current meters, drifters, and shipboard profilers), confirming OSCAR's reliability in capturing time-averaged zonal and meridional currents. Rio et al. (2014) further evaluated OSCAR by comparing it with altimetry-based and in situ datasets, highlighting its effectiveness in representing global ocean circulation patterns. For regional applications, Yu et al. (2019) utilized OSCAR data to examine the seasonal and interannual variability of the Indonesian Throughflow (ITF), demonstrating its effectiveness in capturing major current systems in the Indonesian seas. Given these validations, the use of OSCAR in this study provides a robust approach to analyzing surface current dynamics in the southeastern Indian Ocean, particularly in relation to the SJCC and its interactions with the ITF and the SEC.

To ensure the reliability and accuracy of the analysis, this study uses well-established, widely recognized datasets. The spatial resolution of OSCAR data is $0.25° \times 0.25°$ (ESR, 2022). OSCAR data have been validated against in situ observations and altimeter-derived geostrophic currents, making it a reliable source for studying ocean surface circulation patterns, including the SJCC. Similarly, the sea level anomaly dataset from Copernicus Marine Service has been widely used in ocean circulation and climate variability studies, as it provides accurate sea level measurements derived from multi-satellite altimetry (Le Traon et al., 1998). The data have a resolution of $0.125° \times 0.125°$ (Copernicus Marine Service Information, 2024). RAMA data is obtained from the website https://www.pmel.noaa.gov/. The ERA5 surface wind dataset, also from Copernicus, is one of the most comprehensive global atmospheric reanalysis products, offering high-resolution wind-field data that are crucial for understanding wind-driven ocean currents and coastal upwelling processes (Hersbach et al., 2020). The data have a spatial resolution of $0.25° \times 0.25°$ (Hersbach et al., 2023). To analyze the influence of large-scale climate variability, the study incorporates the NINO 3.4 Index from NOAA's Physical Sciences Laboratory (Rayner et al., 2003) and the DMI from the Japan Meteorological Agency (Saji et al., 1999). These indices are widely used to assess the impact of the ENSO and the IOD on regional and global ocean-atmosphere interactions (Saji et al., 1999; Webster et al., 1999; Trenberth, 1997).

The SJCC was identified each month using two criteria: (i) the occurrence of eastward-flowing surface currents south of Java that advect water from the tropical Indian Ocean, and (ii) the sea level gradient between the southeastern Sumatra region and the Java Sea. The SJCC is considered present when the sea level in the southeastern Sumatra region is higher than in the Java Sea, which favors eastward transport along southern Java, and absent when the gradient is reversed. Anomalous events (e.g., IOD or ENSO years) were detected by directly comparing the monthly patterns with the corresponding climatological fields, rather than subtracting a mean climatology, so that the full seasonal cycle was retained. For validation, daily OSCAR zonal currents (July 2010–July 2011) were compared with RAMA mooring observations at 12°S and 80°E, yielding significant relations that confirm the suitability of OSCAR for representing surface currents in this region. The averaging domain (105°E–114°E, 7°S–9°S) follows the classical definition of the SJCC given by Soeriaatmadja (1957) and encompasses the core of the eastward jet. Although

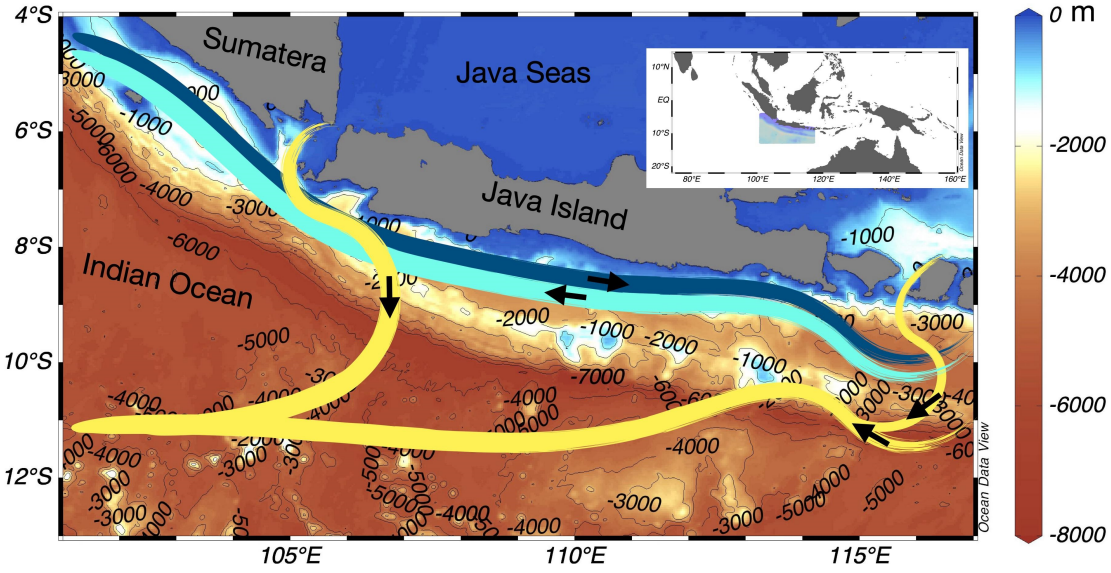

Figure 1. Research location with bathymetry $\frac{1}{2}$ arc second is provided from www.gebco.net. The dark-blue line represents SJC, the light-blue line represents under-SJC, and the yellow line – ITF and SEC. These three main currents are adopted from several findings (Gordon et al., 2010; Iskandar and McPhaden, 2011; Atmadipoera et al., 2022).

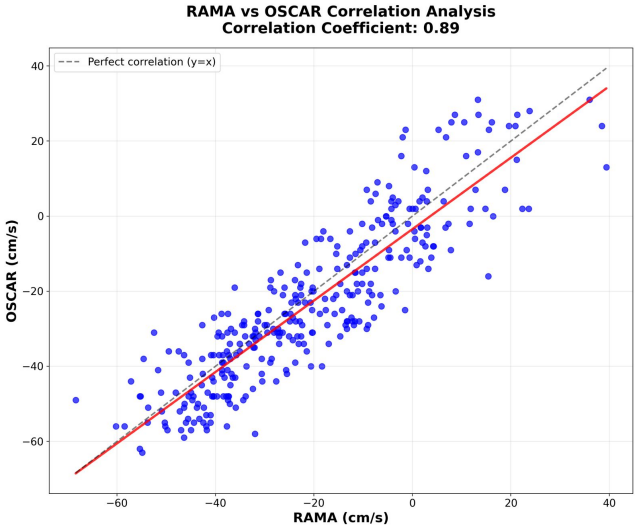

Figure 2. Relation between in situ data from RAMA and OSCAR data.

OSCAR uncertainties are larger near coasts, the agreement with RAMA provides confidence in our estimates. The comparison focused on daily zonal currents at 12°S and 80°E, from 1 July 2010 to 30 June 2011. This analysis assesses how well OSCAR data capture the variability of ocean currents relative to direct observations (Figure 2).

Our findings show that OSCAR zonal currents closely match RAMA observations, with a correlation coefficient of 0.89 and a root-mean-square error of 10.10 cm s^{-1}. These numbers show that OSCAR data offer a reliable picture of daily zonal current fluctuations. While some differences appear at extreme current values, the overall match confirms that OSCAR is a reliable data source for studying ocean current dynamics in this area.

2.3 Analysis

The SJCC was identified each month using two criteria: (i) the presence of eastward surface currents south of Java advecting water from the tropical Indian Ocean, and (ii) the sign of the sea level gradient between the southeastern Sumatra region and the Java Sea. The SJCC is considered present when the sea level in the southeastern Sumatra region is higher than in the Java Sea, which favors eastward transport along southern Java, and absent when the gradient is reversed. Anomalous events (e.g., IOD or ENSO years) were assessed by direct comparison with monthly climatological fields, rather than by anomaly subtraction, to preserve the full seasonal cycle.

Daily OSCAR zonal currents (July 2010–July 2011) were validated against RAMA mooring observations at 12°S and 80°E, showing strong agreement and confirming OSCAR's suitability for representing surface currents in this region. Monthly means of currents, sea level anomaly, and winds were then computed from daily data. All analyses were conducted within 105°E–114°E and 7°S–9°S, consistent with the classical SJCC definition. To distinguish the SJCC from eddy-driven eastward flow, two regimes were defined. The canonical SJCC refers to the seasonal eastward coastal current occurring from October to May, characterized by elevated coastal sea level, sustained eastward zonal velocities, and tropical Indian Ocean water-mass signatures. The event-driven SJCC denotes similar dynamical signatures occurring outside this period, primarily during La Niña or negative IOD events. Regional wind forcing and climate indices (DMI and Niño 3.4) were analyzed to assess their respective roles in modulating SJCC variability (Figure 3).

A clear relationship is observed between strong El Niño events and positive IOD, as in the 1997–1998 and 2015–2016 El Niño episodes, where both indices peaked significantly. Conversely, during La Niña years, such as 2010, the NIÑO 3.4 index dropped. A notable exception to this ENSO-IOD relationship occurred in 2019 when a strong positive IOD developed independently of a major El Niño. While El Niño often drives positive IODs, other atmospheric and oceanic factors can also contribute to their formation. The 2019 event underscores the need for further research into non-ENSO drivers of IOD variability, such as regional wind patterns and ocean-atmosphere feedback mechanisms. Examining the long-term trends, the indices frequently fluctuate above and below the ± 1.0 threshold, marking periods of extreme climate variability. Positive IODs consistently coincide with El Niño phases, whereas negative IODs are less frequently observed during La Niña events.

To distinguish variability across temporal scales, analyses were conducted separately for seasonal, interannual, and subseasonal timescales. Seasonal variability was examined using monthly climatological means of zonal surface currents, sea-level anomalies, and surface winds. Interannual variability was assessed using monthly anomalies relative to the climatology and composited for selected ENSO and IOD events.

To investigate the spatiotemporal evolution of the SJCC and its dynamical forcing mechanisms, Hovmöller diagrams were constructed using sea level anomaly, zonal surface current velocity, and zonal wind stress. The fields were meridionally averaged over the southern Java coastal waveguide (7°–9°S) and plotted as a function of longitude and time. Zonal current Hovmöller diagrams were employed to assess the continuity, persistence, and longitudinal coherence of eastward flow along the southern Java coast, allowing differentiation between the SJCC and short-lived or localized eastward currents. Zonal wind Hovmöller diagrams were analyzed to evaluate the contribution of local wind forcing and its phase relationship with the observed current variability. The combined Hovmöller analysis of SLA, zonal currents, and zonal winds provides a physically consistent framework for distinguishing the coastally trapped SJCC from wind-driven Ekman flows, eddy-induced transport, and transient sea level anomalies.

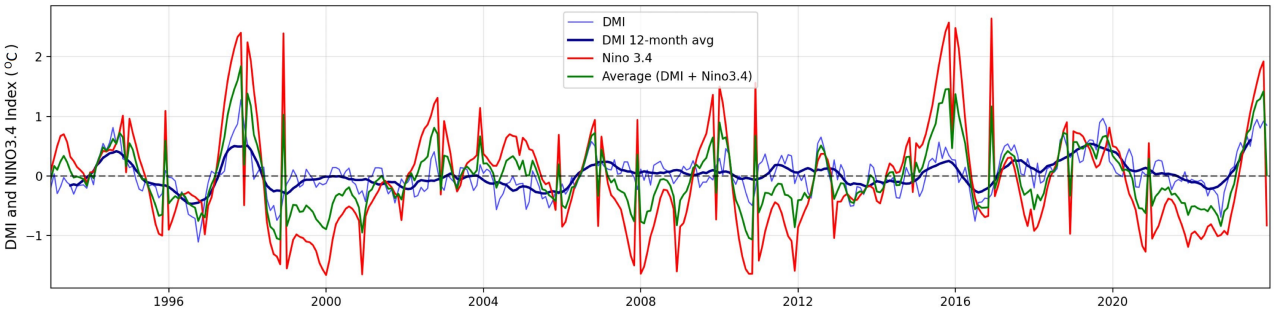

Figure 3. The time series of the Dipole Mode Index (DMI) and the Niño 3.4 Index from 1995 to 2023.

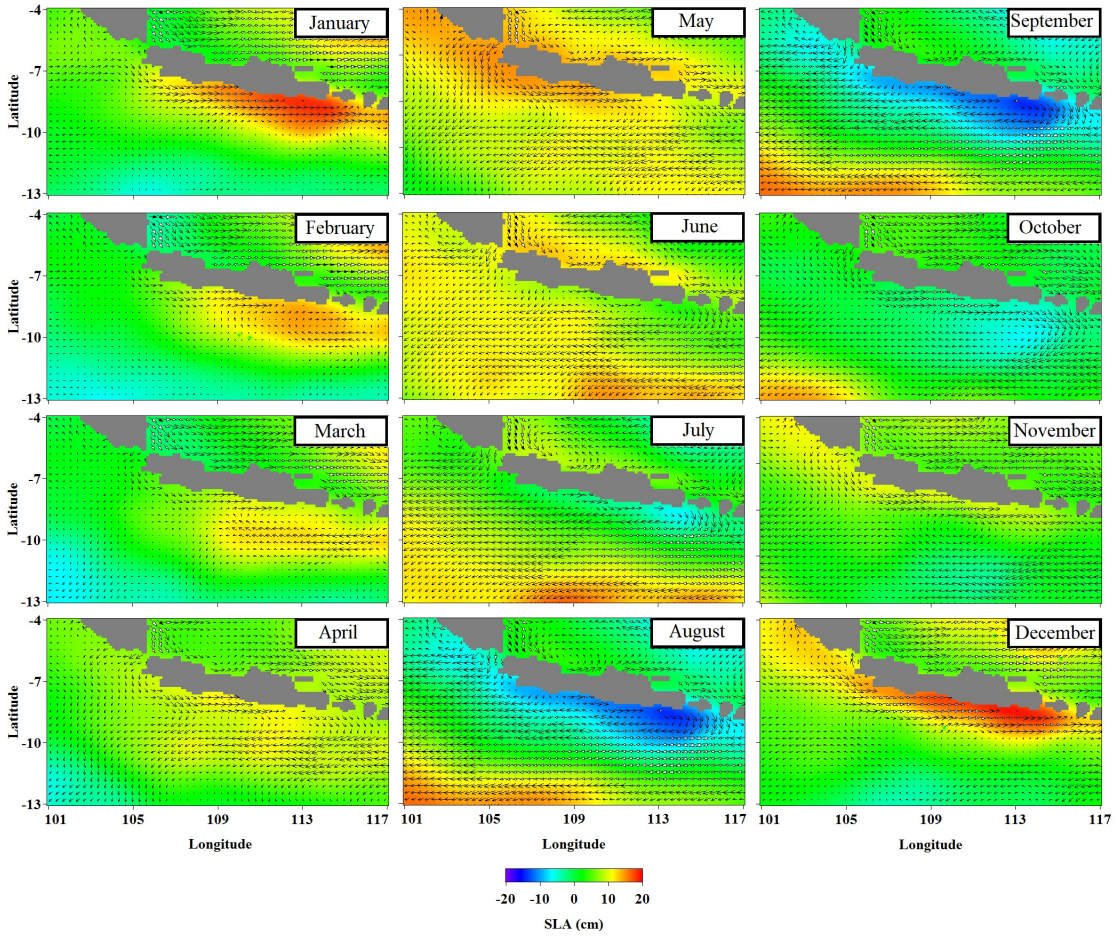

Figure 4. Monthly pattern of surface current circulation (vectors) overlaid with sea level (colours). Grey colours represent island surroundings.

This approach also enables assessment of SJCC modulation under different climate states, including normal years and extreme ENSO and IOD events.

3. Results

3.1 Monthly climatology of ocean currents and wind

Surface circulation and sea level in the southern waters of Java exhibit a pronounced seasonal cycle linked to monsoonal forcing (Figure 4). The eastward surface currents are strongest and most spatially extensive during the boreal winter and transition seasons (October–May), extending from the coastline to ~9°–10°S and accompanied by elevated sea level (up to ~14 cm). During this period, sea level in the southern waters of Java remains predominantly positive, supporting sustained eastward flow along the coast.

The seasonal cycle begins in January, when an elevated sea level (≈13–14 cm) along southern Java supports a well-developed eastward surface current extending offshore

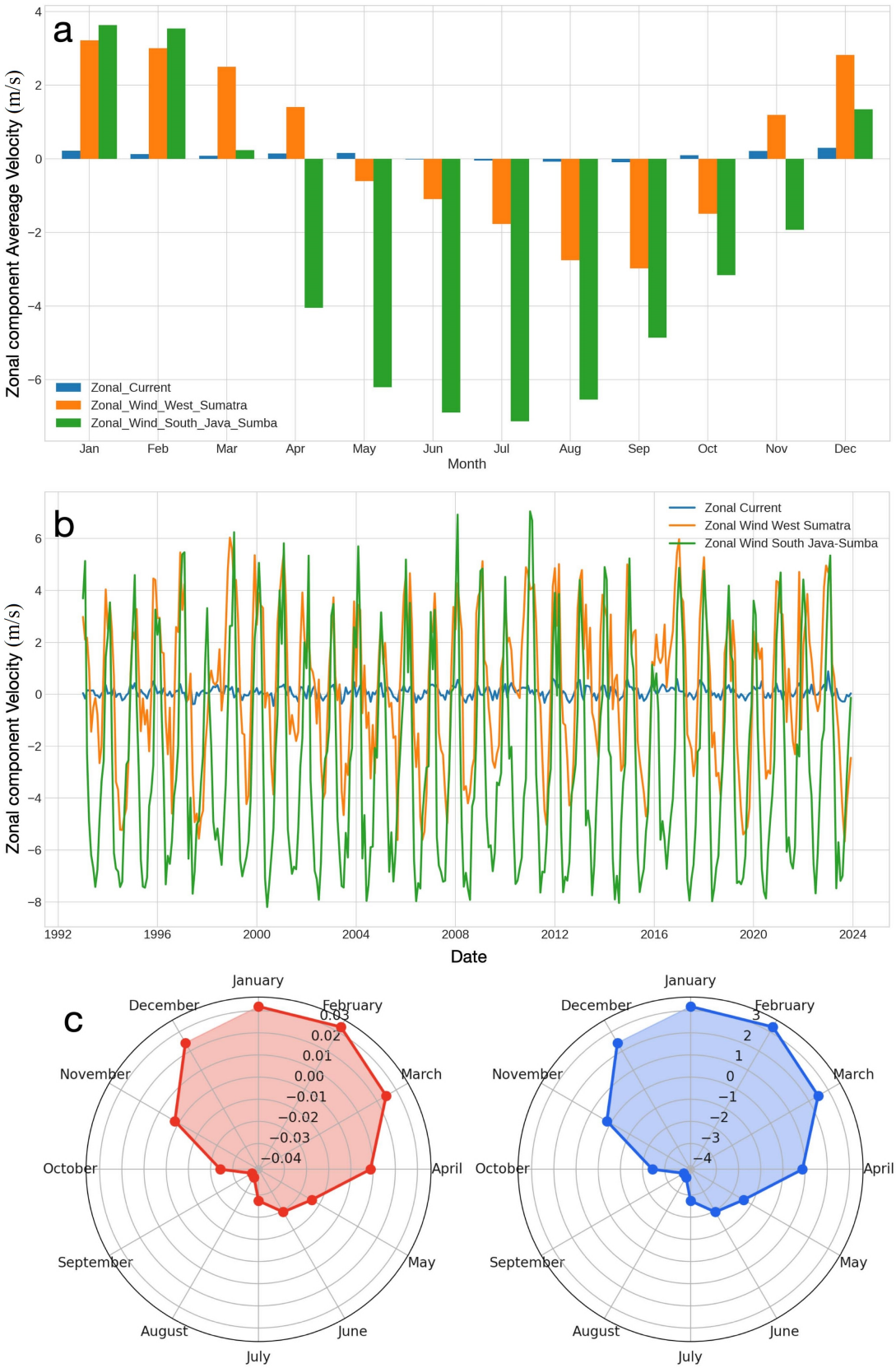

Figure 5. Wind and sea surface currents patterns. a) Monthly zonal currents (blue bars), zonal wind in western Sumatra (orange bars), and zonal wind in southern Java (green bars). b) Zonal wind and currents from 1993 to 2024, c) monthly ocean currents velocity (m/s) and direction (left) and wind (right) velocity and direction.

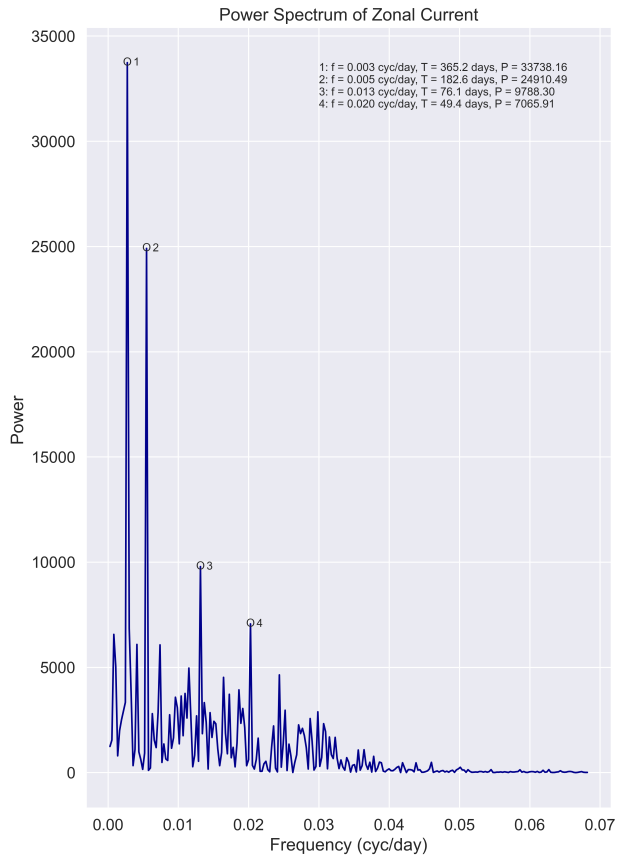

Figure 6. Power spectrum of zonal currents in the southern waters of Java.

to approximately 9°S–10°S. From February to March, the sea level gradually decreases (~8–10 cm), and the eastward surface currents weaken and become more spatially confined, indicating a transition toward monsoon reversal. During April–May, sea level rises again (~10–12 cm), accompanied by renewed and broader eastward surface currents along the southern Java coast. In contrast, during the southeast monsoon period (June–September), sea level drops to near-zero and negative values (down to ~9 cm), and the eastward surface currents are restricted mainly to the central and eastern sectors of southern Java, consistent with intensified upwelling conditions. From October onward, sea level increases rapidly and the eastward surface currents re-establish along the entire southern Java coast, reaching their maximum extent in November–December, when sea level exceeds ~14 cm.

The monthly surface wind patterns over western Sumatra and southern Java reflect the strong influence of the Asian-Australian monsoon system, driving distinct seasonal transitions in the equatorial eastern Indian Ocean (Figure 5). During the northwest monsoon (January–March), winds are generally weak and directed from the northwest to the west over both regions. A transitional phase occurs in April–May, when winds over western Sumatra shift southwestward while southeasterly winds begin to develop along the southern coast of Java. The southeast monsoon (June–August) is characterized by strong, well-organized southeasterly winds along southern Java and east–southeasterly winds west of Sumatra, corresponding to the period of maximum wind intensity. From September to October, wind strength decreases, and directions gradually reverse. By November–December, weak northwestward winds dominate again, marking the re-establishment of wet-season conditions. Average power spectra of zonal currents in the southern waters of Java cover the area of 7°S–9°S and 105°E–114°E (Figure 6). The zonal current spectrum at the intraseasonal timescale shows a dominant significant peak around 76 days.

3.2 Seasonal variability of the eastward surface currents and sea level under IOD conditions

In general, during a negative phase of the IOD, anomalies in sea surface circulation are observed. Under normal conditions from June to September, the eastward surface currents typically form only in the central to eastern parts of southern Java, with relatively limited coverage. In June 2016, however, the eastward surface currents developed along the entire southern coast of Java, with a notably broad extent from the shoreline, reaching as far south as 10.4°S. Sea level in the southern waters of Java rose significantly, reaching approximately 39.10 cm. In July 2016, the eastward surface currents also formed along the southern coast of Java, though with a narrower extent from the coast to 8.9°S, accompanied by a sea level rise of 23.51 cm. In August, the eastward surface currents extended from the coastline to 8.6°S, with sea level increasing to 15.70 cm. Then, in September 2016, the eastward surface currents were again observed, with coverage reaching 9.1°S. The sea level in the southern waters of Java further rose to 22.36 cm (Figure 7).

Under normal conditions, from October to December, the eastward surface currents typically develop along the southern waters of Java, with a broad extent that reaches as far south as 9.7°S. However, during the positive IOD phase, the extent of the eastward surface currents became narrower, accompanied by a decrease in sea level. In October 2019, the eastward surface currents were observed only in the western part of southern Java (107.8°E–110.3°E), extending from the coastline to 8.1°S, with a concurrent sea-level drop of −15.90 cm. In November 2019, the eastward surface currents were confined to the central and eastern regions of the southern waters of Java (107.5°E–112.3°E), with coverage from the coast to just 8.4°S and a sea level of approximately −2.73 cm. In December 2019, the eastward surface currents were observed only in the central southern Java region (107°E–110.3°E), reaching up to 8.1°S, and in the eastern part (110.5°E–114°E), extending up to 8.6°S. By January 2020, the eastward surface currents developed along the entire southern coast of Java,

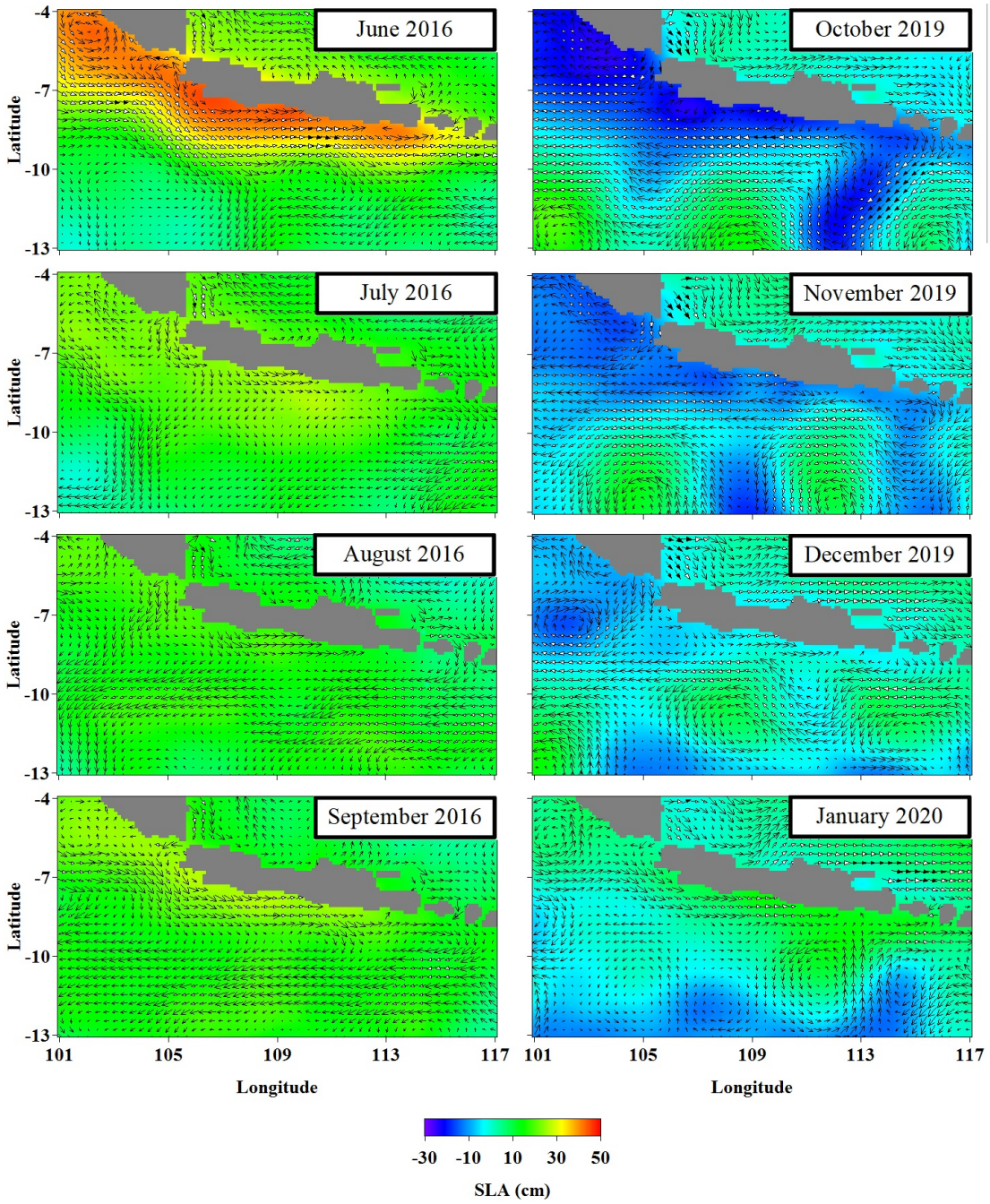

Figure 7. The pattern of sea surface circulation from June to September 2016 during a negative IOD event (left) and October 2019 to January 2020 during a positive IOD event (right). Grey colours represent the island surroundings.

extending from the coastline to 8.9°S, with sea level rising to approximately 9.18 cm.

3.3 Sea surface circulation and sea level variability in southern Java during the 2010 La Niña and 2015 El Niño events

In general, the spatial extent of the eastward surface currents during the La Niña of 2010 was broader compared to normal-year conditions. In June 2010, the eastward surface currents were observed only in the central part of southern Java (108.3°E–110.5°E), extending from the coastline to 8.3°S, with a sea level anomaly of approximately 6.85 cm. In July 2010, the eastward surface current extent widened, with sea level reaching around 6.13 cm. These currents formed in the central-southern waters of the Java region (107°E–110.3°E), extending to 8.4°S, and in the eastern part of southern Java (110.5°E–114°E), reaching 9.1°S. By August 2010, the eastward surface currents

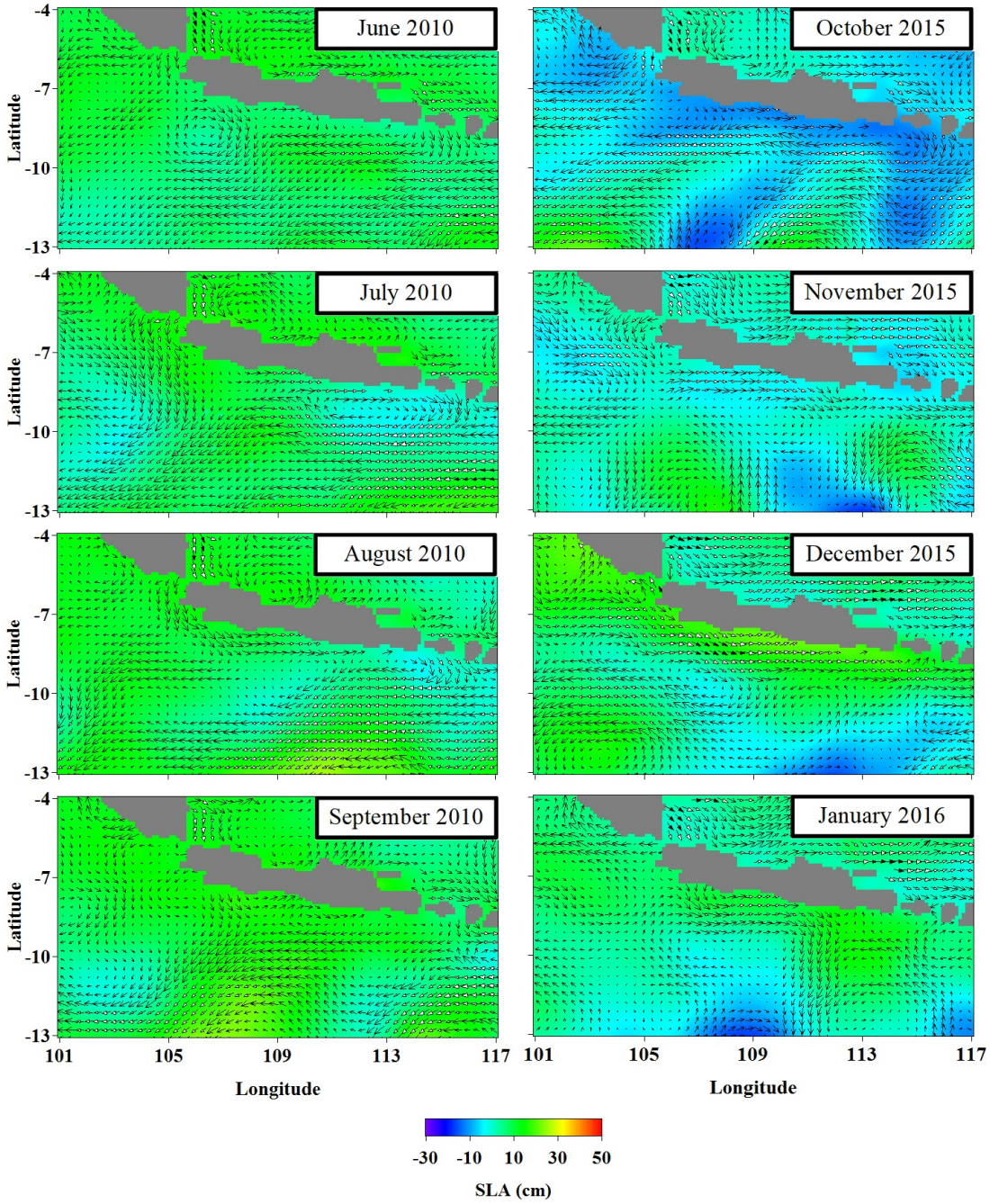

Figure 8. The pattern of sea surface circulation from June to September 2010 during the 2010 La Niña event (left) and October 2015 to January 2016 during the 2015 El Niño event (right). Grey colours represent the island surroundings.

extended along the entire southern coast of Java, reaching 8.6°S, with a sea level of 6.24 cm. In September 2010, the eastward surface currents again extended across the southern waters of Java, from the coastline to 8.6°S, accompanied by a sea-level rise of approximately 13.83 cm (Figure 8).

Overall, during the 2015 El Niño, the spatial extent of the eastward surface currents was narrower than under normal conditions. In October 2015, the eastward surface currents were observed only in the central part of the southern waters of Java (107°E–110.3°E), extending from the coastline to 8.1°S, and in the eastern part of the southern waters of Java (110.5°E–114°E), extending to 8.6°S. The sea level in the southern waters of Java dropped to −9.47 cm. In November 2015, the eastward surface currents formed along the southern coast of Java, from the coastline to 9.1°S, with a sea level anomaly of approximately −1.70 cm. In December 2015, the eastward

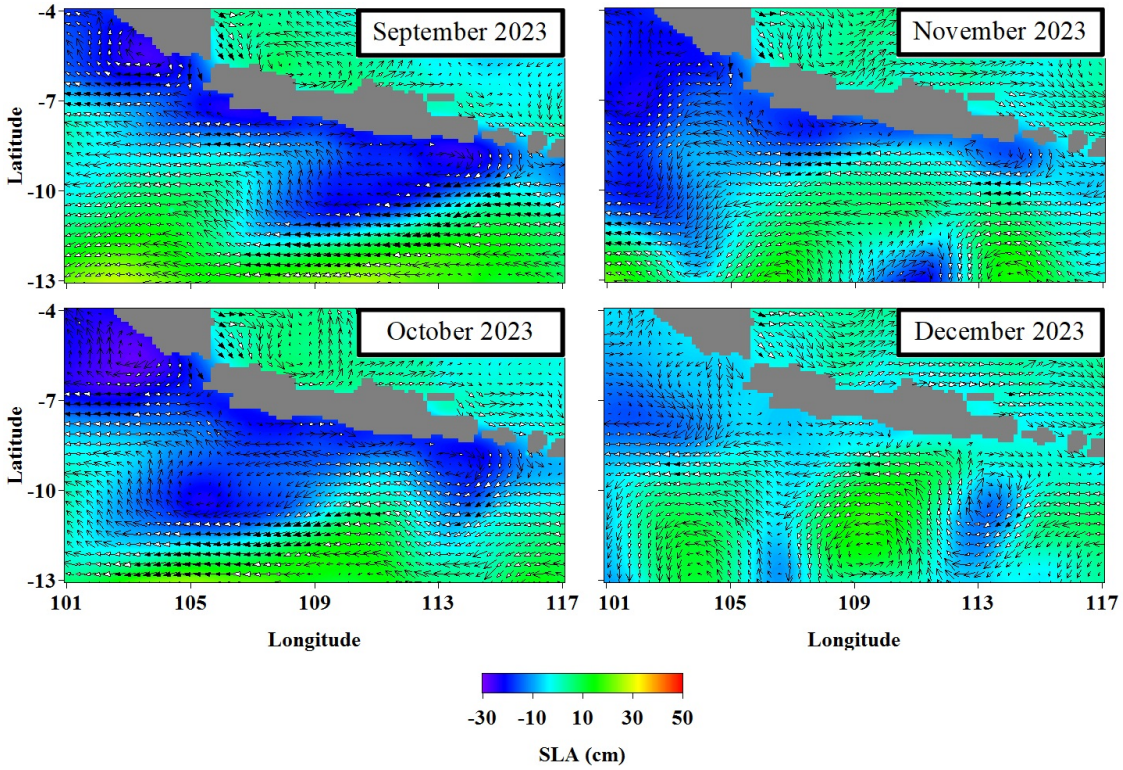

Figure 9. The pattern of sea surface circulation from September to December 2023 during the simultaneous occurrence of a positive IOD and El Niño. Grey colours represent the island surroundings.

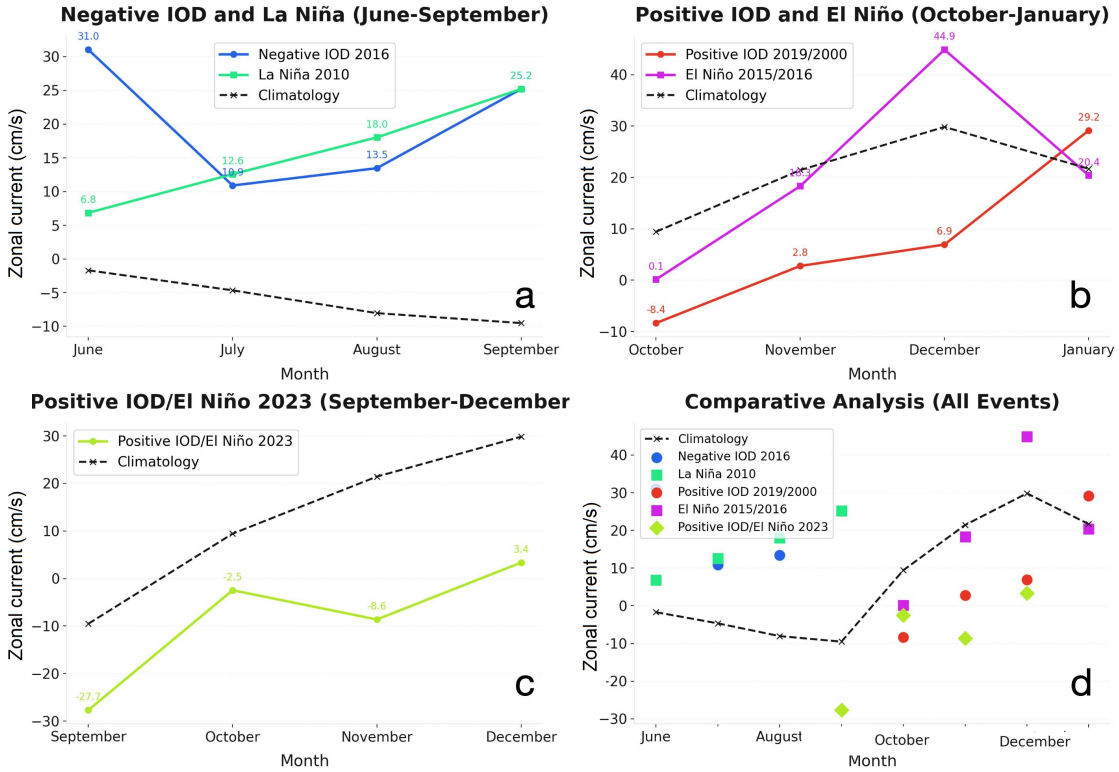

Figure 10. Anomalies of the eastward surface currents from October to January during the 2019 positive IOD and the 2015 El Niño, and IOD/El Niño 2023.

Table 1. Summary of the eastward surface current anomalies, SLA, wind patterns, and significance during major IOD and ENSO events.

Event	Climate mode	Eastward surface current anomaly	SLA patterns	Wind anomaly	Significance
2010 (La Niña)	Negative ENSO	Strengthened the eastward surface currents (June–September)	Elevated SLA	Westerly anomaly	$r = 0.65$, $p < 0.05$
2015 (El Niño)	Positive ENSO	Suppressed the eastward currents (October–January)	Depressed SLA	Easterly anomaly	$p < 0.05$
2016 (−IOD)	Negative IOD	Strengthened the eastward currents (June–September)	Elevated SLA	Westerly anomaly	$p < 0.05$
2019 (+IOD)	Positive IOD	Suppressed the eastward currents (October–January)	Depressed SLA	Easterly anomaly	$p < 0.05$
2023 (+IOD; El Niño)	Combined event	Strong suppression of the eastward currents (September–December)	Strongly depressed SLA	Persistent easterly anomaly	$p < 0.05$

surface currents continued along the southern coast of Java, extending from the coastline to 9.4°S, accompanied by a sea-level rise of around 15.28 cm. By January 2016, the eastward surface currents extended across the southern waters of Java, reaching as far south as 9.5°S, with sea level rising to approximately 9.08 cm.

3.4 Suppression of the eastward surface currents and sea level depression along southern Java during the 2023 positive IOD–El Niño event

In September 2023, the eastward surface currents were observed only in the central part of the southern waters of Java (108.8°E–110°E), extending from the coastline to 8.1°S, and in the eastern part of the southern waters of Java (110.3°E–114°E), extending to 8.6°S (Figure 9).

The sea level in the southern waters of Java dropped to −16.99 cm. In October 2023, the eastward surface currents formed only in the central part of the southern waters of Java (106.8°E–110.3°E), from the coastline to 8.1°S, with the sea level dropping further to approximately −17.32 cm. In November 2023, the eastward surface currents remained limited to the central-southern coast of Java (106.8°E–109.5°E), with a narrower extent that reached only as far south as 7.9°S, and a sea level anomaly of approximately −12.05 cm. By December 2023, the eastward surface currents were still confined to the central-southern waters of the Java region (106.8°E–110°E), reaching as far south as 8.1°S, with a sea level anomaly of around −2.32 cm.

The eastward surface currents have varying responses to climatic patterns. In the context of negative IOD conditions in 2016 and La Niña in 2010, the eastward surface currents intensified from June to September, significantly above the weak climatological normal, signifying an event-driven eastward surface current occurring outside its typical seasonal framework. Conversely, positive IOD events (2019/2000) and El Niño occurrences (2015/2016) from October to January typically inhibited or postponed the eastward surface currents, resulting in diminished eastward surface currents relative to climatological norms. The 2023 concurrent positive IOD–El Niño event exhibited the most significant suppression, with negative anomalies enduring from September to November despite climatological intensification. In summary, negative phases (La Niña, negative IOD) amplify the eastward surface currents, whereas positive phases (El Niño, positive IOD, and their concurrent occurrence) diminish or attenuate them (Figure 10).

Conditions during a negative IOD in 2016 and La Niña in 2010 from June to September are compared with climatology (Figure 10a). The results show that both events produced values well above the climatological norm, with negative IOD 2016 peaking sharply in June (~31.0 cm s^{-1}) and rising again in September (~25.2 c ms^{-1}), while La Niña 2010 displayed a steady increase from June (~6.8 cm s^{-1}) to September (~25.2 cm s^{-1}). This suggests that both negative IOD and La Niña support the enhancement of oceanographic features, such as elevated sea level or strengthening the eastward surface currents. The impact of positive IOD (2019/2000) and El Niño (2015/2016) during the October to January period is notable (Figure 10b). The positive IOD event exhibited a sharp peak in December (~44.9 cm s^{-1}), exceeding climatology, while El Niño 2015/2016 showed a gradual increase, rising from a negative anomaly in October (−8.4 cm s^{-1}) to a positive value (~29.2 cm s^{-1}) in January. While both events show a delayed response relative to climatology, their influence varies across months. Meanwhile, in 2023, this event is characterized by strongly negative anomalies in September (−27.7 cm s^{-1}) and November (−8.6 cm s^{-1}), with only a slight recovery by December (3.4 cm s^{-1}), highlighting its suppressive impact on the eastward currents related

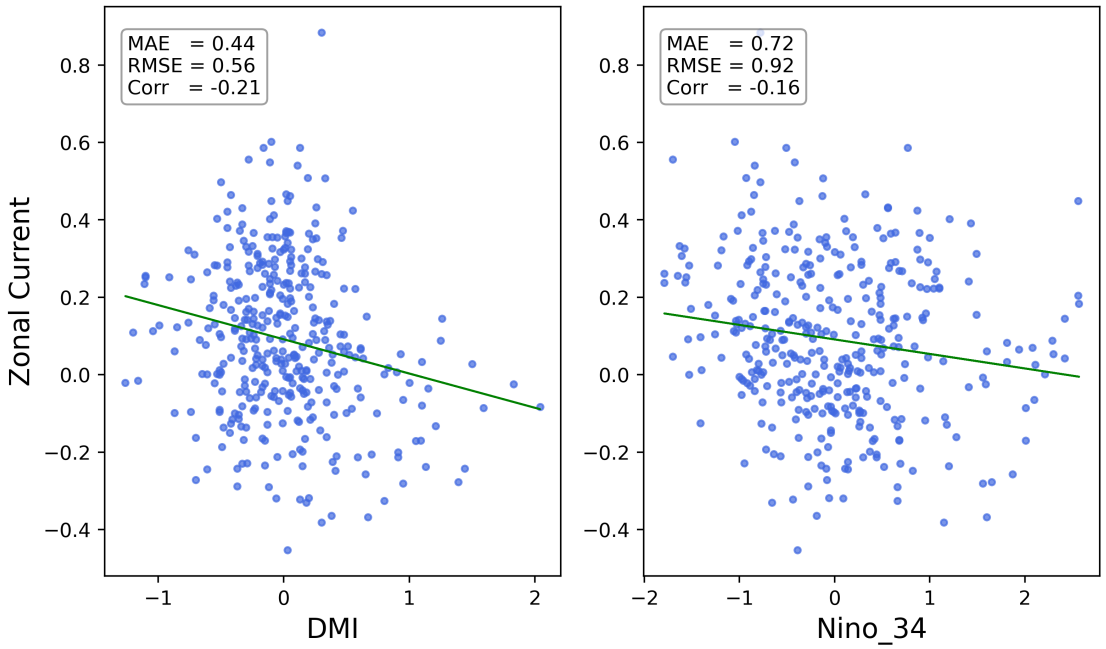

Figure 11. Relation coefficients between zonal current and the DMI index (left) and Niño 3.4 index (right).

variables (Figure 10c). Negative IOD and La Niña events consistently show higher-than-normal values, while positive IOD and El Niño events – especially the 2023 combination – remain below climatology. These results support the conclusion that negative IOD and La Niña events enhance oceanographic activity along the southern coast of Java. At the same time, positive IOD and El Niño suppress it, with IOD exerting a more dominant and immediate influence (Figure 10d). To facilitate comparison across events, the main findings are summarized in Table 1, which lists the associated IOD/ENSO phase, the eastward surface current anomalies, sea level and wind patterns, and statistical significance.

The eastward surface currents exhibit a response significantly modified by large-scale climate patterns. The negative IOD and La Niña episodes in 2010 and 2016 are associated with increased eastward surface currents from June through September, elevated sea levels along the southern coast of Java, and anomalies in westerly winds. In contrast, positive IOD and El Niño events (2015, 2019) result in the suppression of eastward surface currents during October–January, the depression of sea level south of Java, and the presence of easterly wind anomalies. The 2023 combined positive IOD–El Niño event has the highest suppression. It is also characterized by considerable sea level depression and continuous easterly winds. The fact that all of the associations in question are statistically significant, with p-values below 0.05, underscores that these distinctions between events are robust.

The statistical relationship between zonal surface currents south of Java and large-scale climate variability, represented by the DMI and the Niño-3.4 index, is illustrated using scatter plots with linear regression fits and associated error metrics, providing a quantitative assessment of their contemporaneous relationships over the study period (Figure 11). The zonal current exhibits a weak negative relation with the Niño-3.4 index ($r \approx -0.16$), accompanied by a relatively high root mean square error (RMSE ≈ 0.92 m s^{-1}), indicating a large spread of data points around the regression line. In comparison, the relationship between the zonal current and the DMI is also negative but slightly stronger ($r \approx -0.21$), with an RMSE of approximately 0.56 m s^{-1}, reflecting a tighter clustering of the data.

Surface currents flow in the same direction as the local winds only during December–March (eastward) and June–September (westward), indicating periods when the circulation is primarily wind-driven. Zonal winds are predominantly eastward from December to March and westward from April to November (Figure 12). In contrast, during the transition seasons (April–May and October–November), eastward currents persist despite prevailing westward winds. This decoupling between wind direction and current response provides clear evidence of remote oceanic forcing, rather than direct local wind control, governing the circulation along the southern Java coast. The SLA Hovmöller diagram further supports this interpretation. The eastward surface current anomalies are systematically associated with positive SLA anomalies propagating eastward along the coast, whereas westward currents

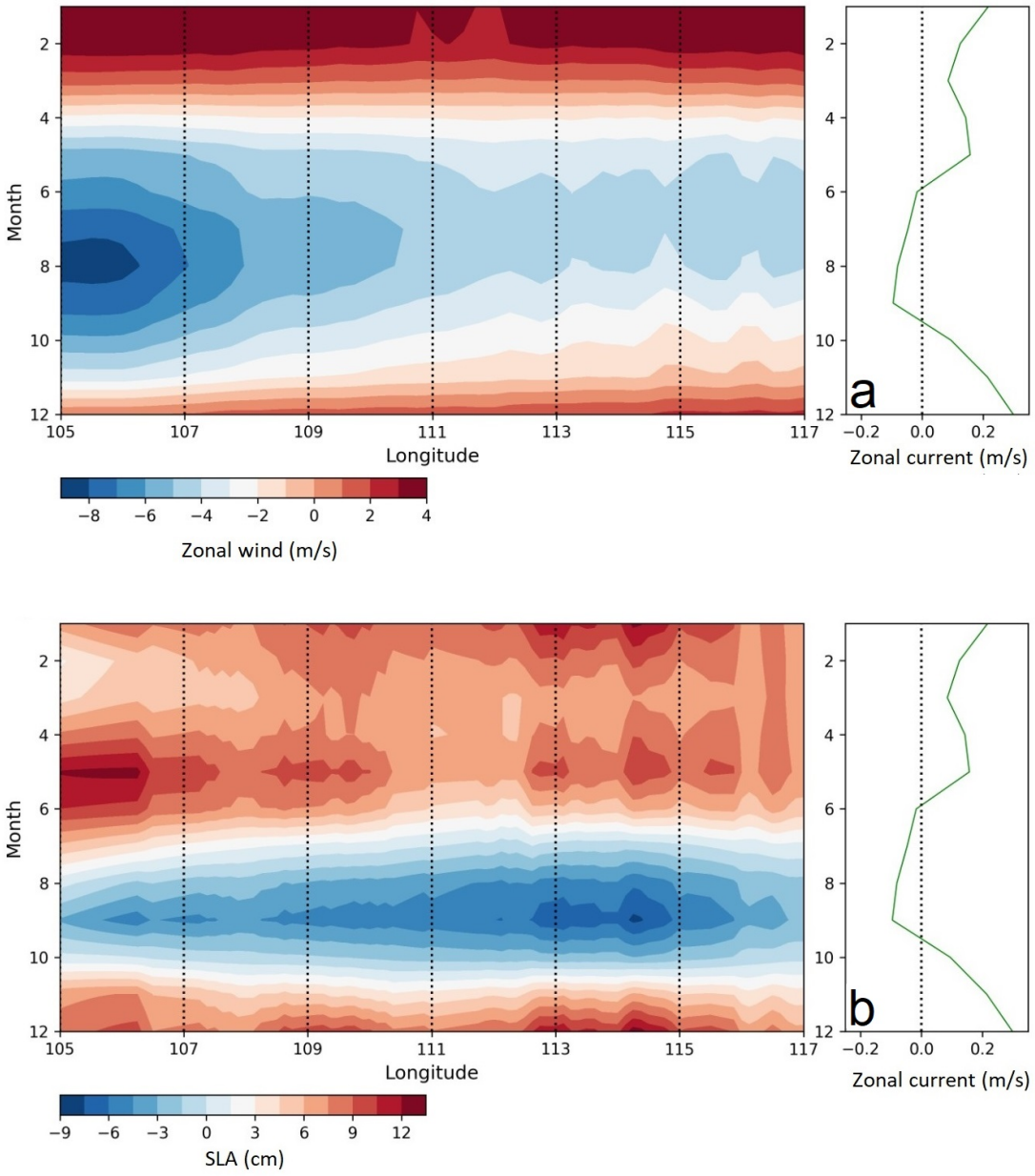

Figure 12. Longitude–time Hovmöller diagrams of a) zonal wind stress, and b) sea level along southern Java.

coincide with negative SLA anomalies. The coherent eastward propagation of positive SLA signals along the southern Java–Sumba waveguide is consistent with coastally trapped Kelvin wave dynamics originating from the equatorial Indian Ocean. These remotely forced waves elevate coastal sea level and drive eastward geostrophic currents, even under unfavorable local wind conditions.

4. Discussion

Analysis results indicate that the eastward surface currents are present throughout the year along the southern coast of Java, albeit with varying spatial extents. This observation is consistent with previous studies showing that the eastward surface current occurs year-round but is governed by different mechanisms (Schott and McCreary, 2001; Sprintall et al., 2010). At intraseasonal time scales, the zonal current spectrum displays a dominant peak at approximately 76 days. This result aligns with several previous studies. Model simulations using the Modular Ocean Model 3 (MOM3) indicate a dominant SJCC variability of around 90 days (Iskandar et al., 2006). Consistently, ADCP measurements at 106.75°E, 8.5°S from December 2008 to May 2010 show that the SJCC varies on a 70–100-day timescale (Utari et al., 2019). These findings highlight the persistent

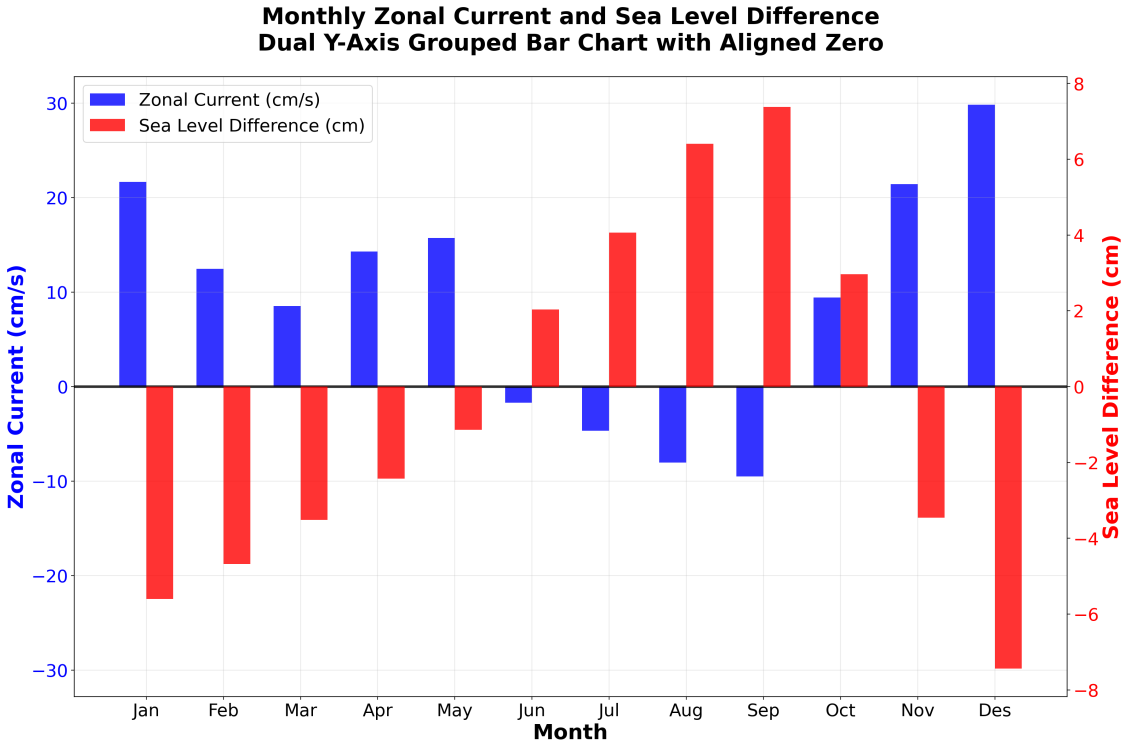

Figure 13. Monthly variations of zonal current and sea level difference.

intraseasonal variability of the SJCC in this region.

A broad eastward surface current, extending from the coastline to 9°S, occurs from October to May, while a narrower current is found from June to September. The zonal current (7°–9°S and 105°–114°E) is closely related to the difference in sea level between the southwestern part of Java (4.6°S–5.8°S and 105.8°E–106.5°E) and the southeastern waters of Sumatra (5.9°S–6.9°S and 104°E–105.1°E). Negative (positive) values indicate that the sea level in the southwestern part of Java is lower (higher) than in the southeastern waters of Sumatra. From November to May (June to October), the sea level in the southeastern waters of Sumatra is higher (lower) than in the southwestern part of Java. When the sea level in the southwest part of Java exceeds that in the southeastern waters of Sumatra, part of the Java Sea current flows into the Indian Ocean through the Sunda Strait, with some of these currents subsequently moving eastward along the southern coast of Java (Figure 13).

Based on Figure 13, the water mass source of the eastward surface current from November to May originates in the tropical Indian Ocean, accompanied by sea level rise along the southern coast of Java. In October, the eastward surface current originates from the tropical Indian Ocean and the southwestern part of Java through the Sunda Strait. Meanwhile, from June to September, the currents that move eastward along the southern coast of Java originate from the southwest of Java, flowing through the Sunda Strait. This finding contrasts with earlier studies, which reported the eastward surface currents forming from November to June (Soeriaatmadja, 1957), from November to April (Wyrtki, 1961), during the northwest monsoon (Gingele et al., 2002; Phillips et al., 2021), or persisting year-round with varying intensity (Schott and McCreary, 2001; Utari et al., 2019). The eastward surface currents exhibit monthly variability in intensity, with the strongest flow occurring from November to January, at 21.4 cm s^{-1}, 29.8 cm s^{-1}, and 21.7 cm s^{-1}, respectively. These results differ slightly from those of Ningsih et al. (2021), who observed a peak in the eastward surface current intensity from December to February. Wijffels et al. (2002) also reported vigorous eastward current intensity in November. In February and March, the eastward surface current intensity declines to 12.5 cm s^{-1} and 8.5 cm s^{-1}. Interestingly, despite the weakening northwest monsoon in April and the emergence of the southeast monsoon in May, SJCC intensity increases to 14.3 cm s^{-1} and 15.7 cm s^{-1}, respectively. Similarly, in October, although the southeast monsoon remains strong, the eastward surface currents begin forming at a speed of 9.4 cm s^{-1}.

In May and October, despite the westerly surface winds over western Sumatra, the eastward surface currents persist. Even in April, when wind speeds are low, and May, when westerlies dominate, the eastward surface currents intensity exceeds that of February, when the northwest monsoon peaks. In October, despite the active southeast monsoon, strong eastward surface currents still develop. This decoupling between local zonal wind forcing and along-

shore current response indicates that the eastward surface currents cannot be explained solely by local wind-driven dynamics. The coherent eastward propagation of positive sea-level anomaly signals along the southern waters of the Java–Sumba coastal waveguide, as revealed by the Hovmöller analysis (Figure 12), is consistent with coastally trapped Kelvin wave dynamics originating in the equatorial Indian Ocean. The propagation slope of sea level anomaly in the Hovmöller diagram corresponds to an eastward phase speed on the order of first-mode coastal Kelvin waves reported in previous studies of the eastern Indian Ocean.

These conditions suggest that, beyond local winds, another forcing mechanism plays a role in the generation of eastward surface currents: the propagation of Kelvin waves from the central tropical Indian Ocean, generated by the eastward Wyrtki Jet (Iskandar et al., 2006; Syamsudin and Kaneko, 2013). Wyrtki Jet intensity peaks during April–May and September–October (Wyrtki, 1973). Periods during which the eastward surface currents occur despite weak or opposing zonal winds (April–May and October–November) therefore reflect a remotely forced oceanic adjustment rather than a direct Ekman response to local winds. This mechanism is believed to strengthen the eastward surface currents in April–May and trigger their formation in October, despite opposing monsoonal winds. The SEC, with its peak intensity in September (Wijffels et al., 1996), may also contribute by reinforcing the Wyrtki Jet and preventing SJCC formation.

Surface winds are a primary driver of ocean surface circulation (Wilson et al., 2016; Dohan, 2017; Röhrs et al., 2021). The positive Indian Ocean Dipole Mode typically develops during the boreal summer monsoon season, driven by negative sea surface temperature anomalies over the tropical southeastern Indian Ocean, which are induced by enhanced alongshore winds off the coasts of Java and Sumatra (Xu et al., 2021). The relation coefficient between the zonal velocity of the eastward surface currents and surface wind velocity is approximately 0.65, with a t-test significance value of around 16.27. It suggests that the eastward surface current dynamics are closely tied to the wind circulation along the western coast of Sumatra. These results align with those of Utari et al. (2019), who reported that eastward surface currents are modulated by local wind forcing.

The surface circulation off southern Java, part of Indonesian waters, is influenced by IOD and ENSO events (Nagura and McPhaden, 2008; Ningsih et al., 2013). During normal years, the eastward surface currents do not form from June to September. During negative IOD events, the intensity of Wrytki Jets in the tropical Indian Ocean intensifies (Srivastava et al., 2025). The strengthening of the Wrytki Jet is indicated as the cause during June to September, under negative IOD and La Niña conditions, with eastward surface currents present. These results are consistent with those of Atmadipoera et al. (2020), who reported that the eastward surface currents were formed during La Niña. The intensity of the SEC in the southeastern part of the Indian Ocean is further strengthened during El Niño and positive IOD events (Chen et al., 2022; Mao et al., 2024). The strengthening of the SEC during positive IOD and El Niño weakens the Equatorial Counter Current. As a source of water mass from the eastward surface currents, the weakening of the Equatorial Counter Current reduces the intensity of the eastward surface currents from October to January during positive IOD and El Niño. Since surface winds drive ocean surface currents, the eastward surface current variations are closely linked to wind dynamics over western Sumatra. Wind anomalies influence zonal surface current circulation (Duan et al., 2016). Typically, westerly winds dominate from June to October. However, during the 2016 negative IOD and 2010 La Niña, winds shifted eastward from June to September. The wind intensity change was more pronounced during the 2016 IOD event than during La Niña. This eastward shift in surface wind direction during June to September is suggested as the driving mechanism for the formation of eastward surface currents during negative IOD and La Niña events.

Under normal-year conditions, the surface wind speed in October was -2.98 m s^{-1}, which significantly increased to -5.29 m s^{-1} during the positive IOD and to -4.70 m s^{-1} during El Niño. In November, surface winds typically shift eastward; however, during both positive IOD and El Niño events, the winds continued to blow westward. In December, surface winds under a positive IOD condition still blew westward, whereas under El Niño, they shifted eastward but weakened in intensity. In January, surface wind intensity was lower during both the positive IOD and El Niño than in the normal year. The increase in surface wind intensity during the 2019 positive IOD was greater than during the 2015 El Niño. Thus, the shift in wind direction and weakening of surface wind intensity off the western coast of Sumatra during the positive IOD 2019 and El Niño 2015 are indicated as the causes of the weakening of the eastward surface currents from October to January.

The surface wind intensity off the western coast of Sumatra from September to December was markedly enhanced during the simultaneous occurrence of positive IOD and El Niño in 2023 compared to climatological normal conditions. Overall, surface wind intensity in September increased from -2.98 m s^{-1} (normal year) to -5.67 m s^{-1} (2023), and in October from -1.49 m s^{-1} (normal year) to -4.24 m s^{-1} (2023). Under normal conditions, surface winds in November and December typically blow eastward, but in 2023, they continued to blow westward. The increased surface wind intensity in September and October 2023, along with the persistent westward wind in November and December 2023, is identified as the cause of the weakening of the eastward surface currents during the simultaneous occurrence of positive IOD and El Niño

in 2023.

The 2023 occurrence, characterized by a positive IOD coinciding with El Niño, resulted in the most significant suppression of the SJCC recorded, with sustained negative anomalies from September to November despite the climatological tendency toward intensification. A direct comparison of individual events (the positive IOD in 2019 and El Niño in 2015) indicates that the suppression in 2023 surpassed that of either phenomenon independently. This indicates a nonlinear compound effect, wherein easterly wind anomalies linked to El Niño intensified those caused by the positive IOD. At the same time, the lack of eastward-propagating Kelvin waves further diminished the SJCC. While a comprehensive dynamical separation of IOD and ENSO influences necessitates more sophisticated statistical methodologies (e.g., partial regression or EOF-based decomposition), which exceed the parameters of this study, our findings underscore that compound climate events may have additional effects on regional circulation beyond simply the aggregation of their individual impacts.

5. Conclusion

The SJCC is an important component of the circulation in the eastern Indian Ocean, influencing water mass transport, upwelling processes, and regional climate variability. Previous studies have shown that the SJCC exhibits significant variability on intraseasonal time scales, which can affect oceanographic conditions along the southern coast of Java. Understanding these variations is crucial for predicting regional ocean dynamics and their impacts on coastal ecosystems. The results show that within the intraseasonal variation, the SJCC has a dominant periodicity of about 76 days. In general, the eastward surface currents along the southern waters of Java form throughout the year, with varying intensities each month. Even though April-May and October-November fall within the southeast season, where surface winds move westward, the intensity of the eastward surface currents is quite strong. The existence and intensity of the eastward surface currents are primarily controlled by surface wind patterns off the western coast of Sumatra and the eastward propagation of equatorial Kelvin waves generated in the tropical western Indian Ocean. Climate modes strongly modulate this system: positive IOD and El Niño events suppress eastward surface currents during their canonical season (October–January), while negative IOD and La Niña conditions promote eastward flow outside this season (June–September). Among these influences, the IOD exerts stronger control on the variability of eastward surface currents than ENSO. The combined positive IOD–El Niño event in 2023 produced the strongest suppression on record, highlighting the nonlinear interactions between climate drivers and underscoring the importance of monitoring variability in eastward surface currents for regional circulation and climate prediction.

Funding

The authors would like to thank the National Research and Innovation Agency (BRIN), which has provided financial support and material assistance to complete this research.

Acknowledgments

The authors would like to thank the PODAAC NASA, PMEL NOAA and Marine Copernicus for providing data access.

Availability of data and materials

All data used are openly available, and relevant websites are mentioned.

Conflict of interest

None declared.

References

Adiwira, H., Purba, N.P., Harahap, S.A., Syamsuddin, M.L., 2018. *Variabilitas suhu laut pada kejadian IOD (Indian Ocean Dipole) di perairan barat Sumatera menggunakan data Argo Float*. Depik 7 (1), 28–41. https://doi.org/10.13170/depik.7.1.8089

Aldrian, E., Susanto, R.D., 2003. *Identification of three dominant rainfall regions within Indonesia and their relationship to sea surface temperature*. Int. J. Climatol. 23, 1435–1452. https://doi.org/10.1002/joc.950

Ashok, K., Guan, Z., Yamagata, T., 2001. *Impact of the Indian Ocean dipole on the relationship between the Indian monsoon rainfall and ENSO*. Geophys. Res. Lett. 28, 4499–4502. https://doi.org/10.1029/2001GL013294

Atmadipoera, A.S., Jasmine, A.S., Purba, M., Kuswardani, A.R.T.D., 2020. UpwellingcharacteristicsinthesouthernJavawatersduringstrongLaNina2010andsuperElŇino2015. Jurnal Ilmu dan Teknologi Kelautan Tropis 12 (1), 257–276. http://doi.org/10.29244/jitkt.v12i1.28977

Atmadipoera, A.S., Koch-Laroy, A., Madec, G., Grelet, J., Baurand, F., Jaya, I., Dadou, I., 2022. *Part I: Hydrological properties within the eastern Indonesian throughflow region during the INDOMIX experiment*. Deep Sea Res. Pt. I, 182 (4), 1–10. https://doi.org/10.1016/j.dsr.2022.103735

Bonjean, F., Lagerloef, G.S.E., 2002. *Diagnostic model and analysis of the surface currents in the tropical Pacific Ocean*. J. Phys. Oceanogr. 32 (10), 2938–2954. https://doi.org/10.1175/1520-0485(2002)032<2938:DMAAOT>2.0.CO;2

Chen, G., Han, W., Wang, D., Zhang, L., Chu, X., He, Y., Chen, J., 2022. *Seasonal structure and interannual variation of the South Equatorial Current in the Indian Ocean*.

J. Geophys. Res.-Oceans 127 (11), 1–13. https://doi.org/10.1029/2022JC018969

Copernicus Marine Service Information, 2024. *SEALEVEL_GLO_PHY_L4_MY_008_047: Global ocean gridded L4 sea surface heights and derived variables reprocessed 1993–ongoing*. EU Copernicus Marine Service (CMEMS), Marine Data Store (MDS). Accessed March 2025.
Available at: https://data.marine.copernicus.eu/product/SEALEVEL_GLO_PHY_L4_MY_008_047

Dohan, K., 2017. *Ocean surface currents from satellite data*. J. Geophys.Res. Oceans, 122, 2647–2651. https://doi.org/10.1002/2017JC012961

Dohan, K., [ESR] 2021. *Ocean Surface Current Analyses Real-time (OSCAR) Surface Currents – Final 0.25 Degree (Version 2.0)* [Data set]. NASA Physical Oceanography Distributed Active Archive Center. Accessed: 2026-04-24
https://doi.org/10.5067/OSCAR-25F20

Duan, Y., Liu, L., Han, G., Liu, H., Yu, W., Yang, G., Wang, H., Wang, H., Liu, Y., Zahid., Waheed, H., 2016. *Anomalous behaviors of Wyrtki Jets in the equatorial Indian Ocean during 2013*. Scientific Reports 6, 29688. https://doi.org/10.1038/srep29688

Feng, M., Wijffels, S., 2002. *Intraseasonal variability in the South Equatorial Current of the east Indian Ocean*. J. Phys. Oceanogr. 32, 265–277. https://doi.org/10.1175/1520-0485(2002)032<0265:IVITSE>2.0.CO;2

Gingele, F.X., Deckker, P.D., Girault, A., Guichard, F., 2002. *History of the South Java Current over the past 80 ka*. Palaeogeogr. Palaeocl. 183 (3–4), 247–260. https://doi.org/10.1016/S0031-0182(01)00489-8

Gordon, A.L., 2005. *Oceanography of the Indonesian seas and their throughflow*. Oceanography 18 (4), 14–27. https://doi.org/10.5670/oceanog.2005.01

Gordon, A.L., Sprintall, J., Van Aken, H.M., Susanto, D., Wijffels, S., Molcard, R., Ffield, A., Pranowo, W., Wirasantosa, S., 2010. *The Indonesian throughflow during 2004–2006 as observed by the INSTANT program*. Dynam. Atmos. Oceans. 50, 115–128. https://doi.org/10.1016/j.dynatmoce.2009.12.002

Hersbach, H., Bell, B., Berrisford, P., Biavati, G., Horányi, A., Muñoz Sabater, J., Nicolas, J., Peubey, C., Radu, R., Rozum, I., Schepers, D., Simmons, A., Soci, C., Dee, D., Thépaut, J.-N., 2023. *ERA5 monthly averaged data on pressure levels from 1940 to present. Copernicus Climate Change Service (C3S) Climate Data Store (CDS)*. Accessed: March, 2025. https://doi.org/10.24381/cds.6860a573

Hersbach, H., Bell, B., Berrisford, P., Hirahara, S., Horányi, A., Muñoz-Sabater, J., Nicolas, J., Peubey, C., Radu, R., Schepers, D., Simmons, A., Soci, C., Abdalla, S., Abellan, X., Balsamo, G., Bechtold, P., Biavati, G., Bidlot, J., Bonavita, M., De Chiara, G., Dahlgren, P., Dee, D., Diamantakis, M., Dragani, R., Flemming, J., Forbes, R., Fuentes, M., Geer, A., Haimberger, L., Healy, S., Hogan, R.J., Hólm, E., Janisková, M., Keeley, S., Laloyaux, P., Lopez, P., Lupu, C., Radnoti, G., de Rosnay, P., Rozum, I., Vamborg, F., Villaume, S., Jean-Noël Thépaut, J.N., 2020. *The ERA5 global reanalysis*. Q. J. Roy. Meteor. Soc. 146 (730), 1999–2049. https://doi.org/10.1002/qj.3803

Hood, R.R., Bange, H.W., Beal, L., Beckley, L.E., Burkill, P., Cowie, G.L., D'Adamo, N., Ganssen, G., Hendon, H., Hermes, J., Honda, M., McPhaden, M., Roberts, M., Singh, S., Urban, E., Yu, Y., 2015. *Science Plan of the Second International Indian Ocean Expedition (IIOE-2): A Basin-Wide Research Program*. Scientific Committee on Oceanic Research, Newark, Delaware, USA. https://archimer.ifremer.fr/doc/00651/76340/77331.pdf

Iskandar, I., McPhaden, M.J., 2011. *Dynamics of wind-forced intraseasonal zonal current variations in the equatorial Indian Ocean*. J. Geophys. Res. 116 (C6), C06019. https://doi.org/10.1029/2010JC006864

Iskandar, I., Tozuka, T., Sasaki, H., Masumoto, Y., Yamagata, T., 2006. *Intraseasonal variations of surface and subsurface currents off Java as simulated in a high-resolution ocean general circulation model*. J. Geophys. Res. 111 (C12), C12015. https://doi.org/10.1029/2006JC003486

Jin, X., Wright, J.S., 2020. *Contributions of Indonesian Throughflow to eastern Indian Ocean surface variability during ENSO events*. Atmos Sci Lett. 21, e979. https://doi.org/10.1002/asl.979

Johnson, E.S., Bonjean, F., Lagerloef, G.S.E., Gunn, J.T., Mitchum, G.T., 2007. *Validation and error analysis of OSCAR sea surface currents*. J. Atmos. Oceanic Tech. 24 (4), 688–701. https://doi.org/10.1175/JTECH1971.1

Kuswardani, R.T.D., Qiao, F., 2014. *Influence of the Indonesian Throughflow on the upwelling off the east coast of South Java*. Chin. Sci. Bull. 59 (33), 4516–4523. https://doi.org/10.1007/s11434-014-0549-2

Le Traon, P.Y., Nadal, F., Ducet, N., 1998. *An improved mapping method of multisatellite altimeter data*. J. Atmos. Ocean. Tech. 15 (2), 522–534. https://doi.org/10.1175/1520-0426(1998)015<0522:AIMMOM>2.0.CO;2

Mao, X., Zheng, S., Feng, M., Liang, P., Xie, L., Yang, L., Yan, L., 2024. *Interannual variability the South Equatorial Current in the Southeast Indian Ocean associated with El Niño-Southern Oscillation*. J. Climate, 38 (3), 545–562. https://doi.org/10.1175/JCLI-D-23-0725.1

Michida, Y., Yoritaka, H., 1996. *Surface currents in the area of the Indo-Pacific throughflow and in the tropical Indian Ocean observed with surface drifters*. J. Geophys. Res. - Ocean, 101 (5). https://doi.org/10.1029/96JC00035

Nagura, M., McPhaden, M.J., 2008. *The dynamics of zonal current variations in the central equatorial Indian Ocean*. Geophys. Res. Lett. 35, L23603. https://doi.org/10.1029/2008GL035961

Ningsih, N.S., Rakhmaputeri, N., Harto, A.B., 2013. *Upwelling Variability along the Southern Coast of Bali and in Nusa Tenggara Waters*. Ocean Sci. J. 48 (1), 49–57. https://doi.org//10.1007/s12601-013-0004-3

Ningsih, N.S., Sakina, S.L., Susanto, R.D., Hanifah, F., 2021. *Simulated zonal current characteristics in the southeastern tropical Indian Ocean (SETIO)*. Ocean Sci. 17, 1115–1140. https://doi.org/10.5194/os-17-1115-2021

Phillips, H.E., Tandon, A., Furue, R., Hood, R., Ummenhofer, C.C., Benthuysen, J.A., Menezes, V., Hu, S., Webber, B., Sanchez-Franks, A., Cherian, D., Shroyer, E., Feng, M., Wijesekera, H., Chatterjee, A., Yu, L., Hermes, J., Murtugudde, R., Tozuka, T., Su, D., Singh, A., Centurioni, L., Prakash, S., Wiggert, J., 2021. *Progress in understanding of Indian Ocean circulation, variability, air–sea exchange, and impacts on biogeochemistry*. Ocean Sci. 17 (6), 1677–1751. https://doi.org/10.5194/os-17-1677-2021

Potemra, J.T., 1999. *Seasonal Variations of upper ocean transport from the Pacific to the Indian Ocean via Indonesian straits*. J. Phys. Oceanogr. 29 (11), 2930–2944. https://doi.org/10.1175/1520-0485(1999)029<2930:SVOUOT>2.0.CO;2

Pranowo, W.S., Kuswardani, A.R.T.D., Nugraha, B., Novianto, D., Muawanah, U., Prihatno, H., Yu, W., 2016. *Ocean-Climate Interaction of South Eastern Indian Ocean for Tuna Fisheries and Its Socio-Economy Impacts*. Int. J. Sci. Res. 5 (4), 1956–1961. https://openknowledge.fao.org/items/d8e50e6e-3359-490b-9ba6-b45ae53ca2c9

Purba, N.P., Khan, A.M., 2019. *Upwelling session in Indonesian waters*. World News of Natural Sciences, 25, 1–10.

Qu, T., Du, Y., Strachan, J., Meyers, G., Slingo, J., 2005. *Sea surface temperature and its variability in the Indonesian region*. Oceanography 18 (4), 50–61. https://doi.org/10.5670/oceanog.2005.05

Quadfasel, D., Cresswell, G.R., 1992. *A note on the seasonal variability of the South Java Current*. J. Geophys. Res. 97 (3685). https://doi.org/10.1029/91JC03056

Rayner, N.A., Parker, D.E., Horton, E.B., Folland, C.K., Alexander, L.V., Rowell, D.P., Kent, E.C., Kaplan, A., 2003. *Global analyses of sea surface temperature, sea ice, and night marine air temperature since the late nineteenth century*. J. Geophys. Res. - Atmospheres, 108 (D14), 4407. https://doi.org/10.1029/2002JD002670

Rio, M.H., Mulet, S., Picot, N., 2014. *Beyond GOCE for the ocean circulation estimate: Synergetic use of altimetry, gravimetry, and in situ data provides the most accurate ocean circulation to date*. Geophys. Res. Lett. 41 (24), 8918–8925. https://doi.org/10.1002/2014GL061773

Röhrs, J., Sutherland, G., Jeans, G., Bedington, M., Sperrevik, A.K., Dagestad, K.F., Gusdal, Y., Mauritzen, C., Dale, A., LaCasce, J.H., 2021. *Surface currents in operational oceanography: Key applications, mechanisms, and methods*. J. Oper. Oceanogr. 16 (1), 60–88. https://doi.org/10.1080/1755876X.2021.1903221

Saji, N.H., Goswami, B.N., Vinayachandran, P.N., Yamagata, T., 1999. *A dipole mode in the tropical Indian Ocean*. Nature 401, 360–363. https://doi.org/10.1038/43854

Schott, F.A., McCreary Jr, J.P., 2001. *The monsoon circulation of the Indian Ocean*. Prog. Oceanogr. 51 (1), 1–123. https://doi.org/10.1016/S0079-6611(01)00083-0

Schott, F.A., Xie, S.P., McCreary, Jr. J.P., 2009. *Indian Ocean circulation and climate variability*. Rev. Geophys. 47, RG1002. https://doi.org/10.1029/2007RG000245

Soeriatmadja, R.E., 1957. *The coastal current south of Java*. Mar. Res. Indonesia, 3, 41–55.

Sprintall, J., Chong, J., Syamsudin, F., Morawitz, W., Hautala, S., Bray, N., Wijffel, S., 1999. *Dynamics of the South Java Current in the Indo-Australian basin*. Geophys. Res. Lett. 26 (16), 2493–2496. https://doi.org/10.1029/1999GL002320

Sprintall, J., Gordon, A.L., Wijffels, S.E., Feng, M., Hu, S., Koch-Larrouy, A., Phillips, H., Nugroho, D., Napitu, A., Pujiana, K., Susanto, R.D., Sloyan, B., Peña-Molino, B., Yuan, D., Riama, N.F., Siswanto, S., Kuswardani, A., Arifin, Z., Wahyudi, A.J., Zhou, H., Nagai, T., Ansong, J.K., Bourdalle-Badié, R., Chanut, J., Lyard, F., Arbic, B.K., Ramdhani, A., Setiawan, A., 2019. *Detecting change in the Indonesian seas*. Front. Mar. Sci. 6, 257. http://doi.org/10.3389/fmars.2019.00257

Sprintall, J., Wijffels, S., Molcard, R., Jaya, I., 2010. *Direct evidence of the South Java Current system in Ombai Strait*. Dynam. Atmos. Oceans, 50 (2), 140–156. https://doi.org/10.1016/j.dynatmoce.2010.02.006

Srivasta, A., Martin, G.M., Pradhan, M., Rao, S.A., Ineson, S., 2025. *The multi-year negative Indian Ocean Dipole of 2021–2022*. EGUshere [preprint]. http://doi.org/10.5194/egushere-2025-2303

Susanto, R.D., Gordon, A.L., Zheng, Q.N., 2001. *Upwelling along the coasts of Java and Sumatra sand its relation to ENSO*. Geophys. Res. Lett. 28 (8), 1599–1602. https://doi.org/10.1029/2000GL011844

Susanto, R.D., Marra, J., 2005. *Effect of the 1997/98 El Niño on chlorophyll a variability along the southern coasts of Java and Sumatra*. Oceanography 18 (4), 24–127. https://doi.org/10.5670/oceanog.2005.13

Syamsudin, F., Kaneko, A., 2013. *Ocean variability along the southern coast of Java and Lesser Sunda Islands*. J. Oceanogr. 69, 557–570.

https://doi.org/10.1007/s10872-013-0192-6

Trenberth, K.E., 1997. *The definition of El Niño*. Bull. Am. Meteor. Soc. 78 (12), 2771–2777. https://doi.org/10.1175/1520-0477(1997)078<2771:TDOENO>2.0.CO;2

Tussadiah, A., Syamsuddin, M.L., Pranowo, W.S., Purba, N.P., Riyantini, I., 2016. *Eddy vertical structure in southern Java Indian Ocean: Identification using Automated Eddies Detection*. Int. J. Sci. Res. 5 (3), 967–971. https:doi.org/10.21274/NOV162003

Utamy, R.M., Purba, N.P., Pranowo, W.S., Suherman, H., 2015. *The Pattern of South Equatorial Current and primary productivity in South Java seas*. [In:] *2015 5th International Conference on Environment Science and Biotechnology (ICESB 2015)*, IPCBEE Vol.81. https://doi.org/10.7763/IPCBEE

Utari, P.A., Setiabudidaya, D., Khakim, M.Y.N., Iskandar, I., 2019. *Dynamics of the South Java Coastal Current revealed by RAMA observing network*. Terr. Atmos. Ocean. Sci. 30 (2), 1–11. https://doi.org/10.3319/TAO.2018.12.14.01

Webster, P.J., Moore, A.M., Loschnigg, J.P., Leben, R.R., 1999. *Coupled ocean-atmosphere dynamics in the Indian Ocean during 1997–1998*. Nature 401, 356–360. https://doi.org/10.1038/43848

Wen, C., Wang, Z., Wang, J., Li, H., Shi, X., Gao, W., Huang, H., 2023. *Variation of the coastal upwelling off South Java and their impact on local fishery resources*. J. Oceanol. Limnol. 41 (1), 1389–1404. https://doi.org/10.1007/s00343-022-2031-3

Wijffels, S.E., Bray, N., Hautala, S., Meyers, G., Morawitz, W.M.L., 1996. *The WOCE Indonesian Throughflow Repeat Hydrography Sections: I10 and IR6*. Int. WOCE Newslett. 24, 25–18. https://oceanrep.geomar.de/id/eprint/5309/1/news24.pdf

Wijffels, S.E., Sprintall, J., Fieux, M., Bray, N., 2002. *The JADE and WOCE I10/IR6 Throughflow sections in the southeast Indian Ocean. Part 1: water mass distribution and variability*. Deep Sea Res. Pt. II, 49 (7–8), 1341–1362. https://doi.org/10.1016/S0967-0645(01)00155-2

Wilson, L.J., Fulton, C.J., McC Hogg, A., Joyce, K.E., Radford, B.T.M., Fraser, C.I., 2016. *Climate-driven changes to ocean circulation and their inferred impacts on marine dispersal patterns*. Global Ecol. Biogeogr. 25, 923–939. https://doi.org/10.1111/geb.12456

Wirasatriya, A., Setiawan, J.D., Sugianto, D.N., Rosyadi, I.A., Haryadi., Winarso, G., Setiawan, R.Y., Susanto, R.D., 2020. *Ekman dynamics variability along the southern coast of Java revealed by satellite data*. Int. J. Remote Sens. 41 (21), 8475–8496. https://doi.org/10.1080/01431161.2020.1797215

Wrytki, K., 1961. *Physical Oceanography of the Southeast Asian Waters*. Naga Rep. Vol. 2. Scripps Inst. Oceanogr., California. https://escholarship.org/content/qt49n9x3t4/qt49n9x3t4.pdf

Wyrtki, K., 1962. *The Upwelling in the Region between Java and Australia during the Southeast Monsoon*. Mar. Freshwater Res. 13 (3), 217–225. https://doi.org/10.1071/MF9620217

Wyrtki, K., 1973. *An equatorial jet in the Indian Ocean*. Science 181, 262–264. https://doi.org/10.1126/science.181.4096.262

Wu, P., Arbain, A.A., Mori, S., Hamada, J., Hattori, M., Syamsudin, F., Yamanaka, M.D., 2013. *The Effects of an Active Phase of the Madden-Julian Oscillation on the Extreme Precipitation Event over Western Java Island in January 2013*. SOLA 9, 79–83. https://doi.org/10.2151/sola.2013-018

Xu, X., Wang, L., Yu, W., 2021. *The unique mean seasonal cycle in the Indian Ocean anchors its various air-sea coupled modes across the basin*. Sci. Rep. 11, 5632. https://doi.org/10.1038/s41598-021-84936-w

Yu, Y., Zhang, D., Lin, X., 2019. *Seasonal and interannual variations of the Indonesian Throughflow derived from OSCAR and reanalysis data*. J. Phys. Oceanogr. 49 (6), 1449–1466. https://doi.org/10.1175/JPO-D-18-0240.1